

## A simple avalanche model for astrophysics and laboratory confinement systems

S. C. Chapman, R. O. Dendy, and B. Hnat

Citation: *Phys. Plasmas* **8**, 1969 (2001); doi: 10.1063/1.1352581

View online: <http://dx.doi.org/10.1063/1.1352581>

View Table of Contents: <http://pop.aip.org/resource/1/PHPAEN/v8/i5>

Published by the [American Institute of Physics](#).

---

### Related Articles

Ring current instabilities excited by the energetic oxygen ions

*Phys. Plasmas* **14**, 092902 (2007)

Quasielectrostatic instabilities excited by energetic oxygen ions in the ring current region

*Phys. Plasmas* **12**, 012903 (2005)

Charge exchange imaging of space plasmas (invited)

*Rev. Sci. Instrum.* **75**, 3526 (2004)

On nonlinear plasma instabilities during the substorm expansive phase onset

*Phys. Plasmas* **11**, 2046 (2004)

Interpretation of Cluster data on chorus emissions using the backward wave oscillator model

*Phys. Plasmas* **11**, 1345 (2004)

---

### Additional information on *Phys. Plasmas*

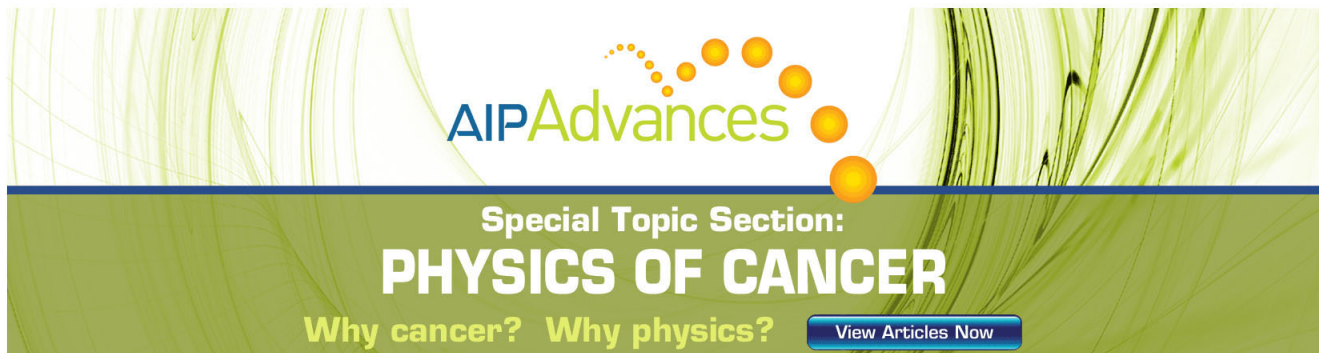
Journal Homepage: <http://pop.aip.org/>

Journal Information: [http://pop.aip.org/about/about\\_the\\_journal](http://pop.aip.org/about/about_the_journal)

Top downloads: [http://pop.aip.org/features/most\\_downloaded](http://pop.aip.org/features/most_downloaded)

Information for Authors: <http://pop.aip.org/authors>

## ADVERTISEMENT



**AIP Advances**

Special Topic Section:  
**PHYSICS OF CANCER**

Why cancer? Why physics? [View Articles Now](#)

# A simple avalanche model for astrophysical and laboratory confinement systems\*

S. C. Chapman<sup>†,a)</sup>

*Space and Astrophysics, Physics Department, University of Warwick, United Kingdom*

R. O. Dendy

*EURATOM/UKAEA Fusion Association, Culham, United Kingdom*

B. Hnat

*Space and Astrophysics, Physics Department, University of Warwick, United Kingdom*

(Received 18 October 2000; accepted 12 December 2000)

An avalanche or “sandpile” model is discussed that generalizes the original self-organized criticality avalanche model of Bak, Tang, and Wiesenfeld [Phys. Rev. Lett. **59**, 381 (1987)] to include spatially extended local redistribution. A single control parameter specifies the spatial extent of local redistribution when the critical gradient is exceeded: this has profound consequences for nonlocal avalanching transport and for the dynamical behavior of the system, which are insensitive to other details such as the initial conditions and fluctuations in fueling or the critical gradient. The model possesses essentially two regimes of behavior. If the scale of nonlocal transport is of the order of the system size, the system is in the vicinity of a fixed point; in consequence the statistics of energy dissipation and length of avalanches are power law, and the time evolution is irregular (“intermittent”). If this scale is significantly smaller than the system size, the time evolution is quasiregular and follows a limit cycle. The first of these regimes appears relevant to the earth’s magnetosphere, where bursty transport and large scale reconfiguration (substorms) are observed. In this case the avalanche statistics have been inferred from observations of patches of intensity in the aurora, which may map to energy dissipation events in the magnetotail. The second regime displays significant links to the observed confinement phenomenology of magnetic fusion plasmas, corresponding to a broader range of model parameter space. For example, there is correlation between sandpile profiles, stored energy, and edge steepening on the one hand, and the control parameter on the other. © 2001 American Institute of Physics. [DOI: 10.1063/1.1352581]

## I. INTRODUCTION

There is growing interest in relating the observed characteristics of energy transport in both astrophysical and laboratory plasmas to “sandpile” models<sup>1</sup> that dissipate energy by means of avalanches. In these models avalanches occur whenever the local gradient is driven above a critical value, triggering local redistribution, which when iterated toward stability produces spatially extended (sometimes global) relaxation events. In drawing parallels with space and laboratory plasmas, there are essentially three points of contact. First, the statistics (magnitude and frequency) of avalanche-type energy release events that are observed in plasma systems may display inverse power law features characteristic of sandpile algorithms. Second, “nonideal” features of the observed plasma event statistics (for example, bumps and bends outside the power law range) may also be recoverable from simple sandpile algorithms. And third, empirical features of a sandpile (for example, the scaling of its profile and energy storage capacity with model parameters) may display significant parallels with those of complex plasma systems.

Interesting questions of a theoretical nature remain in the first area, notably the extent and significance of any link between plasma phenomenology and the scale-free inverse power law statistics that are characteristic of self-organized criticality (SOC),<sup>1,2</sup> which we discuss below; we then focus primarily on the second and third areas outlined above.

In the case of the solar wind-magnetosphere-ionosphere system, the exploration of avalanche models was initiated by the suggestion<sup>3</sup> that the dynamic magnetosphere may be described by an SOC state. Observational motivation was initially provided by power law features of magnetospheric index data, notably AE, which is an indicator of energy dissipated by the magnetosphere into the ionosphere.<sup>4</sup> However, these observations have recently been called into question as an unambiguous indicator (see Refs. 5, 6) so here we discuss more recent evidence which utilizes more direct observation of energy dissipation into the aurora.<sup>7</sup> Importantly, the global disruptions of the magnetotail (substorm events) appear to have occurrence statistics with a well defined mean. There exists a class of sandpile models (e.g., Refs. 8, 9) that yield systemwide avalanches whose statistics have a well-defined mean (intrinsic scale), as well as yielding internal avalanche statistics that are scale free; this motivated both the original application of such models to the global

\*Paper D11 2, Bull. Am. Phys. Soc. **45**, 87 (2000).

<sup>†</sup>Invited speaker.

<sup>a)</sup>Also at Space and Astrophysics, University of Warwick, U.K.

magnetosphere,<sup>10</sup> and the work involving a generalization of the algorithm<sup>11</sup> described below.

An additional issue arises in the coupled solar wind-magnetosphere-ionosphere system, where observations rather than controlled experiments are the available means by which the question of scale free statistics can be investigated. Ideally, one attempts to test unambiguously the hypothesis that the probability distributions of energy dissipated, length scales and durations of events internal to the magnetospheric system (internal avalanches) are inverse power law as expected for a system in SOC;<sup>12</sup> specifically, a slowly driven sandpile. We will discuss how a feature generic to most edge-driven sandpile models is that the index of the power law signature in statistics of energy release events is robust against fluctuations and variations in the mean value of the drive<sup>13,6</sup>—a key requirement for comparison with observations. A generic feature of this type of statistical experimental evidence is that long runs of data are required, and in the magnetospheric system it is unavoidable that both the instantaneous value and the recent mean of the loading rate (the solar wind) will have strong variation.

Interest in applications of the sandpile paradigm to magnetic fusion plasmas was initially motivated in part by observations of rapid nonlocal nondiffusive energy transport events in tokamaks; for early reviews, see, for example, Refs. 14,15. Intriguing observations of such events continue to be made in tokamaks,<sup>16–18</sup> and in large scale numerical simulations thereof.<sup>19,20</sup>

In parallel, a more general physics question has also been implicit (and sometimes explicit) in many studies. Namely, the extent to which other salient features of observed tokamak confinement phenomenology—the result of complex interplay between many plasma processes operating on many length scales and time scales—may also emerge from simple sandpile-type algorithms. We shall explore this question in Sec. IV. For completeness, we also note that the sandpile/SOC paradigm has found application to the primary naturally occurring instance of toroidal magnetized plasmas, namely astrophysical accretion disks; see, for example, Refs. 21–23.

Let us now introduce the general properties of a simple new sandpile model<sup>11</sup> which incorporates previous models<sup>1,8</sup> as limiting cases. We shall then review its potential relevance for the dynamics of the coupled solar wind-magnetosphere-ionosphere (notably the results of Ref. 7) and for laboratory plasmas (examined in greater detail in Ref. 24).

## II. THE SANDPILE ALGORITHM

The sandpile is represented by a one-dimensional grid of  $N$  equally spaced cells one unit apart, each with sand at height  $h_j$ , and local gradients  $h_j - h_{j\pm 1}$ . A repose gradient  $z_R$  is specified below which the sandpile is always stable (the heights  $h_j$  and the local gradients are measured relative to this). A critical gradient  $z_c$  is also specified and in the results presented here this is random;  $z_c = \langle z_c \rangle \pm \alpha R$  where  $R = [0,1]$  is a uniform random deviate and the system has been investigated for values of  $\alpha$  spanning three orders of magni-

tude, here,  $\alpha = 1$ . If the local gradient exceeds  $z_c$  the sand is redistributed to neighboring cells and iteration produces an avalanche. The average magnitudes of  $z_c$  and  $z_R$  simply scale the total amount of sand and energy in the system.

Sand is added to this edge driven sandpile at the closed boundary cell 1 at a constant inflow rate  $g = 1$  (to which we have normalized the  $h_j$  and time). The inflow rate is small compared to the inter-avalanche time, i.e.,  $z_c/g \gg 1$  and the dynamics is found to be insensitive to  $z_c$  and  $g$  provided that this condition holds; here we will show results for  $\langle z_c \rangle = 100$ . As soon as the critical gradient is exceeded the sand is redistributed. The redistribution rule is conservative and instantaneous: avalanches are evolved until at all cells the local gradient is below the critical gradient and only then is further sand added. At each iteration within an ongoing avalanche the height of sand behind the unstable site is reduced so as to flatten a “flowing” region  $L \leq L_f$  back to the angle of repose; this sand is relocated to the next cell. The flowing region includes all sites behind the unstable site up to either the sandpile boundary or to maximum value  $L_f$ , whichever is smaller,  $L_f$  is then the fixed control parameter for a given sandpile model.

The edge of an ongoing avalanche then propagates forwards from one cell ( $k$ ) to the next ( $k+1$ ) if

$$h_k - h_{k+1} > z_c. \quad (1)$$

This results in a quantity of sand  $\Delta$  being deposited on the next cell (where \* indicates intermediate steps in the relaxation):

$$h_{k+1}^* = h_{k+1} + \Delta, \quad (2)$$

such that the gradient at cells  $k-i$ ,  $i=0, L-1$  relaxes to the angle of repose (here normalized to zero)

$$h_{k-i}^* - h_{k+1-i}^* = z_R = 0, \quad i=0, L-1, \quad (3)$$

by conservatively removing sand

$$h_{k-i}^* = h_{k-i} - \frac{\Delta}{L}, \quad i=0, L-1. \quad (4)$$

Equations (2)–(4) uniquely specify  $\Delta$ . Backward propagation of the avalanche edge (from  $k$  to  $k-1$ ) then occurs if  $h_k - h_{k-1} > z_c$  and is achieved by the same redistribution rule, that is, by adding sand  $\Delta$  to cell  $k-1$  that has been removed conservatively from cells  $k+i$ ,  $i=0, L-1$ .

An avalanche may be entirely an internal rearrangement of sand or may continue until it spreads across all  $N$  cells of the pile (a system wide discharge), in which case we apply open boundary conditions  $h_N^* = h_N = 0$ .

The total energy dissipated by avalanche events (both internal and systemwide) is just given by the difference in the potential energy in the entire sandpile “before” and “after” the avalanche:

$$d\epsilon = \sum_{j=1}^N h_j^2 \Big|_{\text{after}} - \sum_{j=1}^N h_j^2 \Big|_{\text{before}}. \quad (5)$$

A major feature of this relaxation rule is that it enforces a minimum length scale  $L_f$  for propagation of information (correlation). The model combines the dynamics of ava-

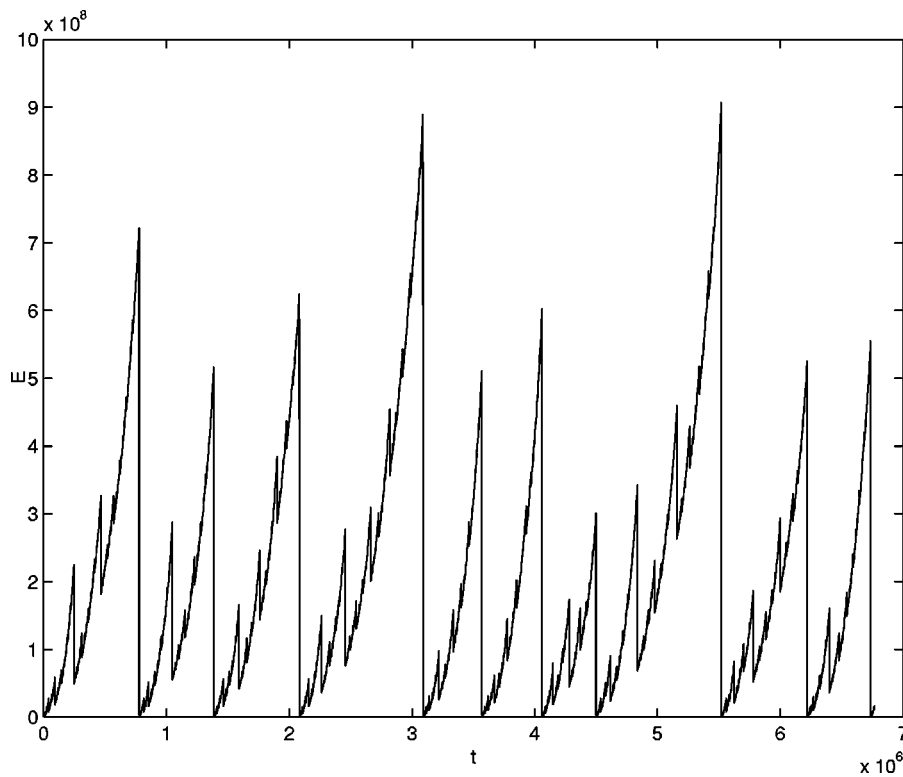


FIG. 1. The time evolution of energy in a 4096 cell sandpile, with  $L_f=N$ .

lanching through the inclusion of a critical gradient with a flowing region where redistribution occurs although the local gradient is less than critical.

The boundary conditions effectively drive the system at short spatial scales and remove fluctuations at the largest spatial scales; instability will always first occur at cell 1 and then can extend over a region of between 1 and  $N$  cells in length, whereas only avalanches of the length of the system will interact with the outflow boundary.

The parameter  $L_f/N$  essentially controls the dynamical behavior of the system. The special case  $L_f=1$  corresponds to the trivial fixed point of the traditional BTW (Bak, Tang and Wiesenfeld<sup>1</sup>) sandpile edge driven in one dimension; in this case the sandpile reaches a unique equilibrium configuration in which the gradients at all cells are just at critical. All avalanches are  $N$  cells in length and consist of each added “grain” of sand propagating from the top to the bottom of the pile. The other limit  $L_f=N$  has been shown to correspond to a nontrivial (repulsive) fixed point<sup>25</sup> by application of a real space renormalization group analysis. The RG procedure extracts scaling laws as scale lengths  $L \rightarrow \infty$  and thus analytically provides the scaling for large scale internal avalanches; here predicting a power law of index  $-1$  which is found in both the statistics of lengths and energy released by internal avalanches.<sup>26,11</sup>

A typical time series for the energy is shown in Fig. 1 for the case  $L_f=N$ . The 4096 cell sandpile was loaded slowly ( $g=1$ ) wrt the mean value of the  $z_{c,j}=100$  and  $\alpha=0.01$ . Here the angle of repose is normalized to zero; the time evolution may then be characterized by a systematic growth as sand is added, interspersed with system wide avalanches where the energy falls back to zero, and internal

avalanches where the energy is reduced to some nonzero value.

The system is close to the vicinity of the nontrivial fixed point for a range of  $L_f \sim N$ ; as evidenced by power law probability distributions of index  $-1$ .<sup>11</sup> The time series of such a case, with  $L_f=1000$  in an  $N=4096$  system is shown in Fig. 2; dynamically this is similar to the  $L_f=N$  case. Specifically, the indicator of the dynamical properties of these systems found in the range  $L_f \sim N/4 - N$  is that a small change in the level of fluctuations on the critical gradient,  $\alpha$ , produces strongly diverging time series which have (numerically) indistinguishable probability distributions for avalanche lengths and energy release (see Ref. 11 for details).

An example of dynamics far from the  $L_f=N$  fixed point is given in Fig. 3. Here  $L_f=50$  (all other parameters unchanged from the previous plots) and the probability distribution of internal avalanche lengths exhibits power law slope  $-1$  over a restricted range corresponding to small avalanches of length  $L < L_f$ .<sup>11</sup> The system dynamics for  $L_f \ll N$  is now quasiperiodic (although each point in Fig. 3 corresponds to an avalanche). In addition, the dynamics in the time domain can be distinguished from that of the  $L_f \sim N$  systems by its robustness against varying the fluctuation level  $\alpha$ ; the time series do not diverge for different fluctuation levels.

We will now explore the relevance of these different regimes of behavior for plasma confinement systems: the earth’s magnetosphere, and for tokamaks.

### III. THE DYNAMIC MAGNETOSPHERE

In order to compare the dynamics of avalanche models with the coupled solar wind-magnetosphere we first consider

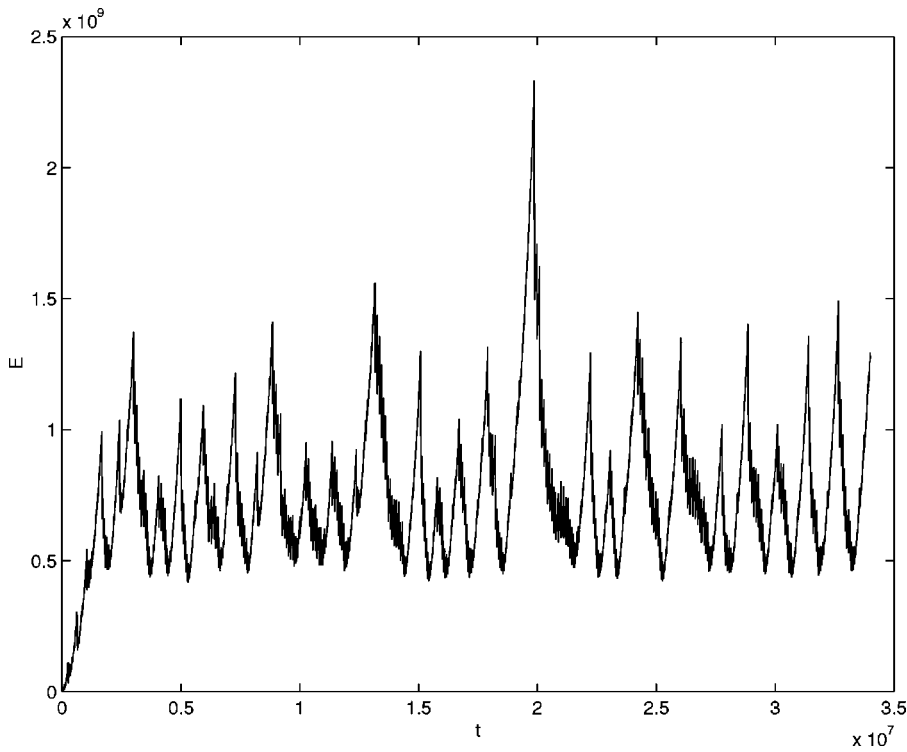


FIG. 2. The time evolution of energy in a 4096 cell sandpile, with  $L_f = 1000 \sim N$ .

the effect of variable drive rate  $g$  (for details see Ref. 13). There are three characteristic time scales implicit in any edge driven sandpile algorithm for such a system: the relaxation time  $\tau_r$  over which an avalanche takes place; the average time required, following an avalanche, for instability to recur at cell 1,  $\tau_u$ ; and the iteration time step  $\Delta t$ . It is clear that  $\tau_u \sim \langle z_c \rangle / \langle g \rangle$  and hence, for instantaneously relaxing sandpile models ( $\tau_r \ll \Delta t$ ) we identify slow and fast loading regimes:

$$\text{slow: } \tau_r \ll \Delta t \ll \tau_u, \tag{6}$$

$$\text{fast: } \tau_r \ll \tau_u \sim \Delta t, \tag{7}$$

respectively. In the latter case, instability is likely to be triggered at each time step. Normalizing  $\Delta t$  to unity, that is one time step occurs in unit time, the fast loading condition becomes  $\langle g \rangle \sim \langle z_c \rangle$ . For any loading rate there is an effective minimum avalanche length required to dissipate the energy

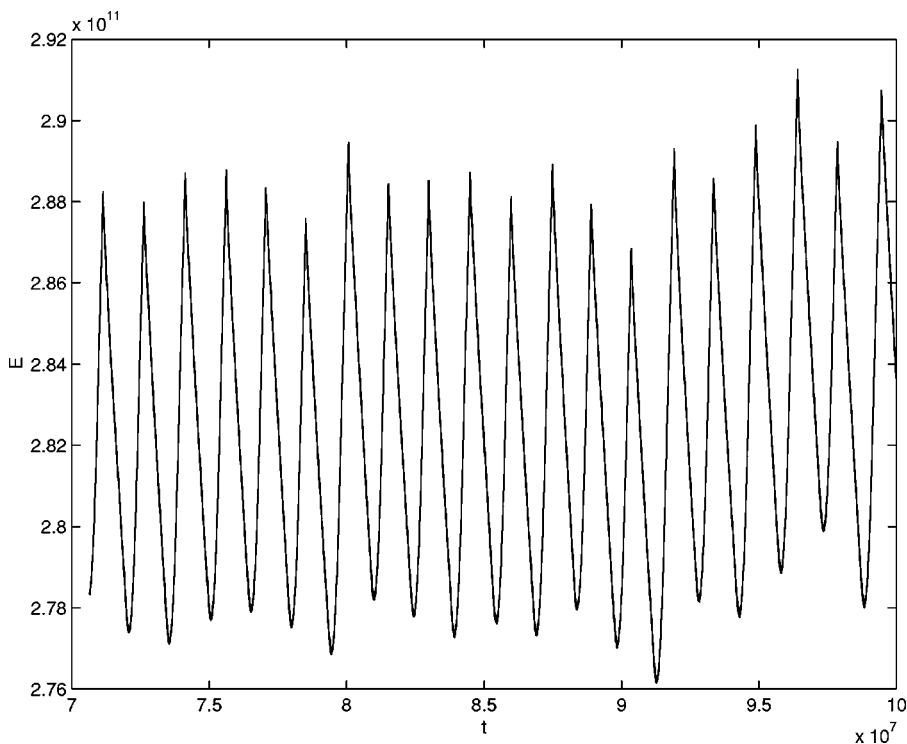


FIG. 3. The time evolution of energy in a 4096 cell sandpile, with  $L_f = 50 \ll N$ .

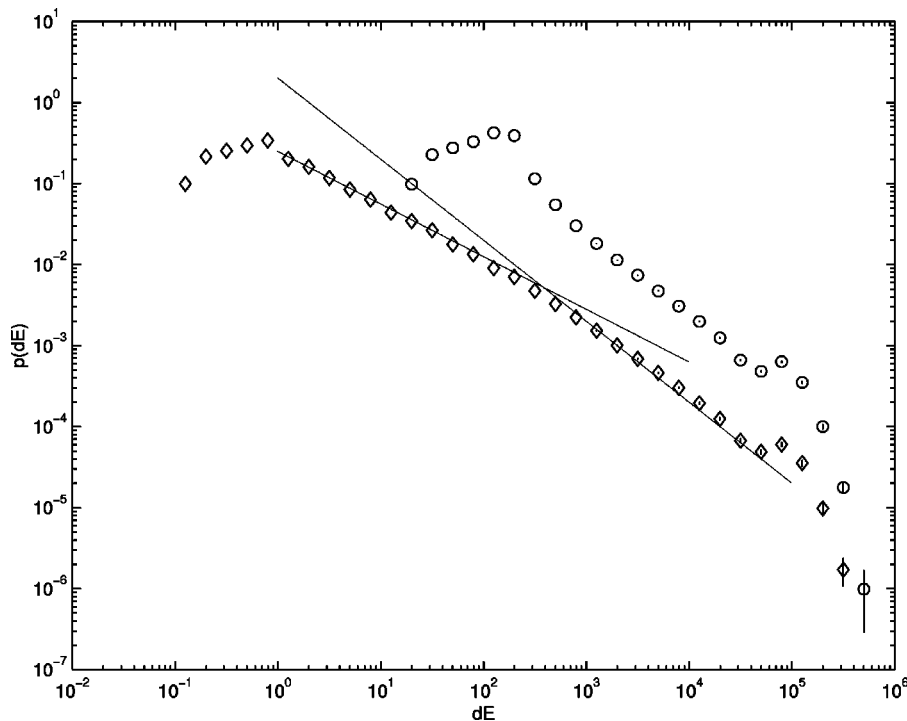


FIG. 4. The probability density of all avalanches for a 5000 cell sandpile with fueling as above ( $\diamond$ ) and the mean fueling rate ten times larger ( $\circ$ ).

associated with the sand added in each  $\Delta t$ . In the slow limit this corresponds to less than one cell, in the fast limit to many. If the mean fueling rate  $\langle g \rangle$  is increased towards and beyond  $\langle z_c \rangle$ , the smallest scale avalanches will be increasingly eliminated. This will be reflected in the lower bound of any range of “power law” event statistics for energy release in the system.

This is illustrated in Fig. 4, which shows the probability distributions for energy released by all avalanches (internal and system wide) in an  $L_f = N$  system for the above inflow rate, and an inflow rate increased by a factor of 10.

The system wide event statistics (the “bump” at largest energy) remain unaffected by the fast loading, illustrating the fact that large avalanches are “well insulated” against the fueling process; however, the internal avalanche distribution displays a dropout in the number of the smallest events. In the case of constant loading there is a sharp cutoff at  $\Delta E \sim 100$  and events below this size are of low probability. Above this, the emergent power law form of the energy release distribution is preserved up to  $\Delta E$  of  $10^5$ . The effect of variability is to “soften” the peak at  $\Delta E$  of 100, and to leave some avalanches down to  $\Delta E = 10$ . The large scale internal avalanches, that is, those governed by the repulsive fixed point, are thus in a sufficiently large system robust against variation in the drive.

We will now attempt a comparison with observed patchy energy dissipation in the magnetosphere. Global “snapshot” images of the entire auroral oval are routinely imaged in the UV by the POLAR UVI instrument; these show resolvable patches of luminosity on scales  $\sim 10$  km to substorm associated activity that spans the entire auroral oval. The size and integrated power of these patches can be extracted from each image by background subtraction and thresholding,<sup>7</sup> the resulting probability distribution of these are found to be in-

sensitive to the threshold level. Results shown in Fig. 5 are for analysis for the entire data set of January 1–31, 1997, consisting of 9033 frames of auroral images. The data are split into “quiet” and “active” intervals corresponding to times when substorm activity was absent, and was found in the interval when the image was taken, respectively. The total number of auroral blobs is 81 794 for quiet time and 155 347 for substorm intervals. We sort the distributions in five bins per decade. The upper range of the area is limited by the total viewing scope of the instrument while the lower range by the instrument’s spatial resolution and sensitivity.

We then see a “bump” in the tail of the distribution corresponding to substorm events which dominate the auroral oval. Intriguingly, during these active times the system still generates structures on smaller scales which lie on a power law distribution. Within statistical fluctuations in the histograms, the indices of these power laws are the same as those which essentially characterize all events occurring in the absence of substorms. We now consider the implications of the conjecture that these patches of auroral emission can be identified with energy dissipation events (avalanches) within the magnetotail. The individual POLAR UVI snapshots provide statistics of the instantaneous distributions of the blobs rather than statistics of their duration; the latter cannot be unambiguously obtained from these data as it would require the identification of specific patches from one frame to the next as they both move and change in time. However, in a system near criticality, the statistics of the spatial distribution of patches of activity is expected to be power law, and to have an index that is related to those of the event lifetimes and total energy dissipated (see, for example, Ref. 12). It should be stressed that this correspondence is not unique to SOC, being a property of other classes of high dimensional nonlinear systems. A characteristic property of

Auroral Blob Analysis from Polar UVI (Jan 1-31, 1997)

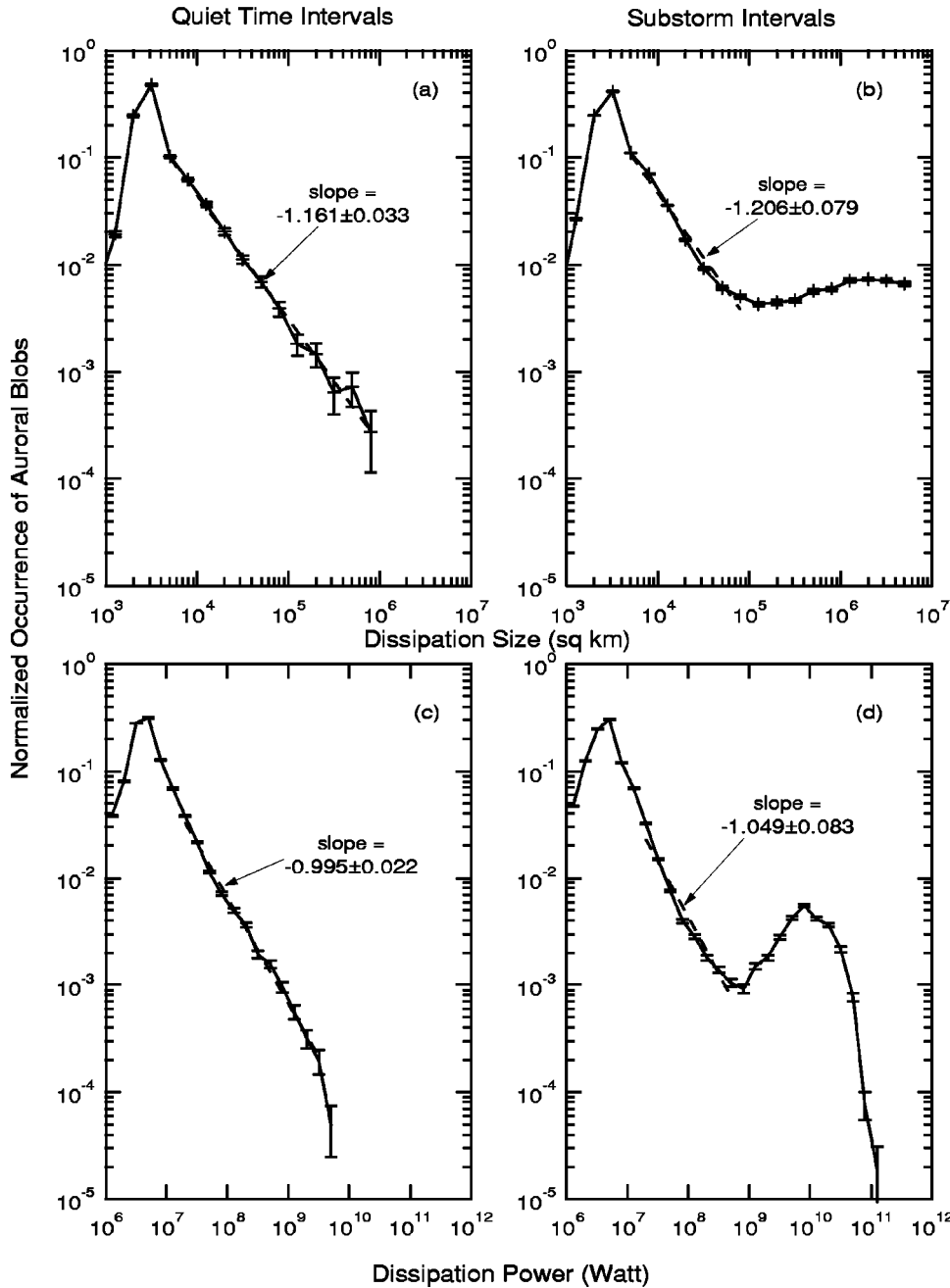


FIG. 5. The probability density of size, and integrated intensity, of patches of activity in the aurora as seen by POLAR UVI [after Lui *et al.*, (2000)].

systems that are critical (in the sense that they are in the vicinity of a nontrivial fixed point identified by RG as discussed here) is that all these statistics are robust against fluctuations in the critical gradients. We have explored this point with a simple sandpile model which has the property that a single parameter  $L_f$  indicates whether the system is close to a nontrivial fixed point. The statistics of large internal events are then found to be power law over their full range, with an index that is robust against variation in the rate of addition of sand, and the value of  $L_f$  for a large range of  $L_f \sim N$ . This suggests that the POLAR UVI analysis supports the original conjecture<sup>3</sup> that the magnetosphere is (in the RG sense) in the vicinity of a nontrivial fixed point.

IV. VARIABLE  $L_f$  AND TOKAMAKS

Recently, we have found significant qualitative parallels between aspects of the observed phenomenology of magnetic fusion plasma confinement systems and the analogous outputs of the model with variable  $L_f$ . We refer to Ref. 24 for a detailed account of current work, which extends to such questions as the correlation between confinement enhancement and edge localized mode (ELM) frequency. Here we focus on one readily obtained observable, namely the average height profile of the simple sandpile model. This is shown in Fig. 6 for an  $N=512$  system, for values of  $L_f$  that explore the range of dynamics discussed above. These pro-

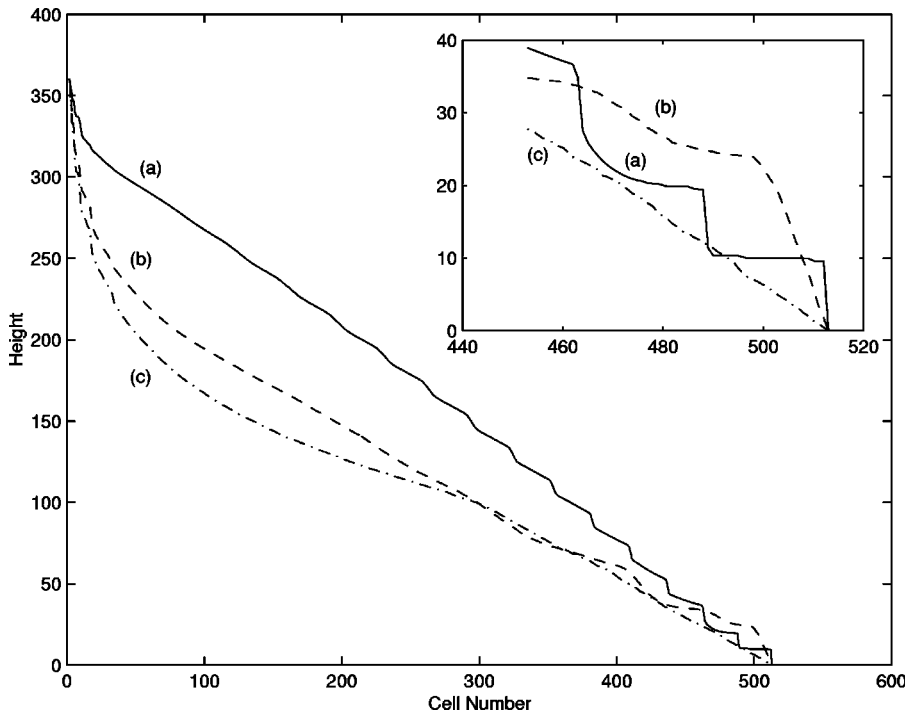


FIG. 6. Time averaged height profile of the sandpile for  $L_f=50$  (a), 150 (b) and 250 (c) for a sandpile of length  $N=512$ .

files are time averaged over many thousands of avalanches and are shown for three different values of  $L_f$  in the range  $50 < L_f < 250$ . The sandpile profile shape, stored gravitational potential energy, and edge structure (smooth decline or pedestal) correlate with each other and with  $L_f$ . As  $L_f$  is reduced, the edge pedestal steepens and the time averaged stored energy rises; multiple steps (regions of steep gradient) are visible in trace (a) and to some extent trace (b). By varying a single parameter, this extremely simple model thus generates features that have more than superficial similarity to, for example, the range of temperature profiles obtained during a JET discharge reproduced from the work of Conway *et al.*<sup>27</sup> in Fig. 7. This similarity appears to have deeper ramifications, which we explore elsewhere.<sup>24</sup>

**V. CONCLUSIONS**

We have outlined the properties of a simple 1.5 D avalanche (“sandpile”) model that exhibits complex dynamics which may be relevant to large scale (astrophysical) and smaller scale (laboratory) magnetized plasma confinement systems. The sandpile model dynamics are specified by the control parameter  $L_f/N$ , which determines whether the system is in the vicinity of a repulsive fixed point. If so, the probability distribution of energy release events and avalanche lengths due to internal reorganization is power law. System wide discharges (flow of “sand” out of the system) form a distinct group which in contrast have a probability distribution with a well-defined mean. The fueling or loading of the system (in the case of the magnetosphere, due to the solar wind) is often characterized by both strong variability about the mean, and a large dynamic range of mean energy input. The inverse power law form of the sandpile statistics has been shown to be robust under fast and/or variable loading. The effect of increased loading rates is to exclude events which dissipate smaller amounts of energy, hence the sandpile tends to yield a single inverse power law regime with turn off at lower energies. One would then expect inverse power law avalanche distributions to be a persistent feature in long runs of data that include “fast” inflow conditions; and this is found to be the case in analysis of power dissipation and size of patches of activity seen in the earth’s auroral oval; see, for example, Figs. 4 and 5 and Ref. 7. The apparent relevance to magnetic fusion plasmas of sandpile model regimes with smaller  $L_f/N$  lies primarily in the emergence of correlations between global confinement, profiles, and edge gradients previously known only from tokamaks; see, for example, Figs. 6 and 7 and discussed further in Ref. 24.

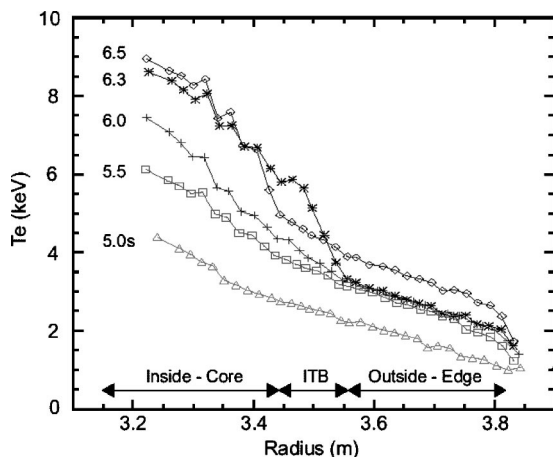


FIG. 7. Radial temperature profiles measured with a 48 channel heterodyne ECE radiometer at different times during a complex evolving JET discharge [see Conway *et al.* (1999)].



## ACKNOWLEDGMENTS

S.C.C. was supported by a PPARC lecturer fellowship, R.O.D. by UK DTI and Euratom, and B.H. by HEFCE.

We are grateful to A. T. Y. Lui and G. Conway for supplying Figs. 5 and 7, respectively.

- <sup>1</sup>P. Bak and C. Tang, Phys. Rev. Lett. **59**, 381 (1987).
- <sup>2</sup>E. Lu, Phys. Rev. Lett. **74**, 2511 (1995).
- <sup>3</sup>T. S. C. Chang, IEEE Trans. Plasma Sci. **20**, 691 (1992).
- <sup>4</sup>G. Consolini in *Proc. vol. 58*, "Cosmic Physics in the Year 2000," edited by S. Aiello, N. Iucci, G. Sironi, A. Treves, and U. Villante (Societa Italiana di Fisica, Bologna, Italy, 1997), 123.
- <sup>5</sup>M. P. Freeman, N. W. Watkins, and D. J. Riley, Geophys. Res. Lett. **27**, 1087 (2000).
- <sup>6</sup>S. C. Chapman and N. W. Watkins, Space Sci. Rev. **95**, 293 (2001).
- <sup>7</sup>A. T. Y. Lui, S. C. Chapman, K. Liou, P. T. Newell, C.-I. Meng, M. J. Brittnacher, and G. K. Parks, Geophys. Res. Lett. **27**, 911 (2000).
- <sup>8</sup>R. O. Dendy and P. Helander, Phys. Rev. E **57**, 3641 (1998).
- <sup>9</sup>S. T. R. Pinho and R. F. S. Andrade, Physica A **255**, 483 (1998).
- <sup>10</sup>S. C. Chapman, N. W. Watkins, R. O. Dendy, P. Helander, and G. Rowlands, Geophys. Res. Lett. **25**, 2397 (1998).
- <sup>11</sup>S. C. Chapman, Phys. Rev. E **62**, 1905 (2000).
- <sup>12</sup>H. J. Jensen, *Self-Organized Criticality: Emergent Complex Behavior in Physical and Biological Systems* (Cambridge University Press, Cambridge, 1998).
- <sup>13</sup>N. W. Watkins, S. C. Chapman, R. O. Dendy, P. Helander, and G. Rowlands, Geophys. Res. Lett. **26**, 2617 (1999).
- <sup>14</sup>D. E. Newman, B. A. Carreras, P. H. Diamond, and T. S. Hahm, Phys. Plasmas **3**, 1858 (1996).
- <sup>15</sup>R. O. Dendy and P. Helander, Plasma Phys. Controlled Fusion **39**, 1947 (1997).
- <sup>16</sup>B. A. Carreras, B. van Milligen, M. A. Pedrosa, R. Balbin, C. Hidalgo, D. E. Newman, E. Sanchez, M. Frances, I. Garcia-Cortes, J. Bleuel, M. Ender, S. Davies, and G. F. Matthews, Phys. Rev. Lett. **80**, 4438 (1998).
- <sup>17</sup>T. L. Rhodes, R. A. Moyer, R. Groebner, E. J. Doyle, R. Lehmer, W. A. Peebles, and C. L. Rettig, Phys. Lett. A **253**, 181 (1999).
- <sup>18</sup>P. A. Politzer, Phys. Rev. Lett. **84**, 1192 (2000).
- <sup>19</sup>X. Garbet and R. Waltz, Phys. Plasmas **5**, 2836 (1998).
- <sup>20</sup>Y. Sarazin and P. Ghendrih, Phys. Plasmas **5**, 4214 (1998).
- <sup>21</sup>S. Mineshige, M. Takeuchi, and H. Nishimori, Astrophys. J. Lett. **435**, L125 (1994).
- <sup>22</sup>K. M. Leighly and P. T. O'Brien, Astrophys. J. Lett. **481**, L15 (1997).
- <sup>23</sup>R. O. Dendy, P. Helander, and M. Tagger, Astron. Astrophys. **337**, 962 (1998).
- <sup>24</sup>S. C. Chapman, R. O. Dendy, and B. Hnat, "A sandpile model with tokamaklike enhanced confinement phenomenology," Phys. Rev. Lett. (in press).
- <sup>25</sup>S. Tam, T. S. Chang, S. C. Chapman, and N. W. Watkins, Geophys. Res. Lett. **27**, 1367 (2000).
- <sup>26</sup>S. C. Chapman, R. O. Dendy, and G. Rowlands, Phys. Plasmas **11**, 4169 (1999).
- <sup>27</sup>G. D. Conway, B. Alper, D. V. Bartlett, D. N. Borba, M. G. von Hellerman, A. C. Maas, V. V. Parail, P. Smeulders, and K.-D. Zastrow, *Proceedings of the 26th European Physical Society Conference on Controlled Fusion and Plasma Physics, Maastricht 1999* (European Physical Society, Petit-Lancy, 1999), p. 177.